

Beam Imaging and Luminosity Calibration

June 14, 2016

Markus Klute, Catherine Medlock, Jakob Salfeld-Nebgen
Massachusetts Institute of Technology

We discuss a method to reconstruct two-dimensional proton bunch densities using vertex distributions accumulated during LHC beam-beam scans. The x - y dependencies in the beam shapes are studied and an alternative luminosity calibration technique is introduced. We demonstrate the method on simulated beam-beam scans and estimate the uncertainty on the luminosity calibration associated to the beam-shape reconstruction to be below 1%.

1 Introduction

During the LHC Run-1 period, the LHC experiments introduced the Van-der-Meer (VdM) [1, 2] scan method for luminosity scale calibration at the hadron collider [3, 4, 5, 6, 7].

The VdM scan method is intended to measure the overlap integral O_I of the colliding proton beams with proton densities ρ_1 and ρ_2

$$O_I = \int_{-\infty}^{\infty} \rho_1(x, y) \rho_2(x, y) dx dy, \quad (1)$$

after integration over the longitudinal coordinate and time. If N_1 and N_2 are the number of protons in the two colliding bunches respectively the instantaneous luminosity can be measured directly from machine parameters according to

$$\mathcal{L} = N_1 N_2 \nu_{\text{rev}} O_I. \quad (2)$$

The measurable rate of a luminometer is given by the luminosity and the visible cross section for a specific luminometer

$$R = \sigma_{\text{vis}} \cdot \mathcal{L}. \quad (3)$$

The VdM scan method relies on the assumption that the bunch proton densities are factorizable in the coordinates, x and y , of the transverse plane of the detector, i.e. $\rho_i(x, y) = \rho_i(x) \rho_i(y)$. In general, this assumption does not hold and introduces one of the leading systematic uncertainties for luminosity calibration measurements [4, 7].

The transverse beam-shape reconstruction therefore poses a challenging problem in the luminosity scale calibration procedure of the LHC experiments. The LHCb collaboration exploits beam-gas interactions to reconstruct the individual proton bunch densities [6, 8, 9]. Another approach exploits the evolution of the mean and width of the luminous region during the beam-beam scans [10]. In addition, a dedicated tailoring of the LHC proton bunch injection chain was investigated to prevent the emergence of non-gaussian beam-shapes [11].

In this paper a method to estimate the x - y dependencies is developed and a new proposal for a complementary luminosity calibration is presented. The method generalizes the beam imaging technique proposed in [12] and experimentally realized in [13, 14] to two dimensions.

In contrast to the standard VdM scan, beam-beam scans with one beam fixed in the rest-frame of the detector per x and y scan are utilized. The distributions of reconstructed proton-proton collision vertices in the transverse plane accumulated during the scans constrain the two-dimensional proton densities and are fitted simultaneously to extract the analytical form for the proton densities of the two beams. As a result,

O_I can be computed and used to estimate the instantaneous luminosity independent of x - y dependencies in the proton densities.

This paper is organized as follows: In Section 2 the impact of dependencies on the standard VdM scan method is studied. In Section 3 a new approach to reconstruct the beam-shapes is introduced and tested on simulated beam-beam scans. In Section 4, a potential bias on the beam overlap estimation is studied and a correction based on a specific regression is applied.

2 Impact of X-Y Dependencies on the VdM Standard Analysis

In this section the impact of x - y dependencies in the LHC bunch proton densities on the standard VdM scan method is demonstrated. A set of simulated VdM scans based on double gaussian beam-shapes for each beam b_i is generated.:

$$b_i(x, y) = w_i g_{i,N}(x, y) + (1 - w_i) g_{i,W}(x, y). \quad (4)$$

Each beam is a sum of a "narrow" gaussian component g_N and a "wide" gaussian component g_W , where each is of the following form:

$$g_{i,j}(x, y) = \frac{1}{2\pi\sigma_{i,j,x}\sigma_{i,j,y}\sqrt{1-\rho_{i,j}^2}} \exp\left(\frac{-1}{2(1-\rho_{i,j}^2)}\left[\frac{x^2}{\sigma_{i,j,x}^2} + \frac{y^2}{\sigma_{i,j,y}^2} - \frac{2\rho_{i,j}xy}{\sigma_{i,j,x}\sigma_{i,j,y}}\right]\right). \quad (5)$$

x - y dependencies, or non-factorizability of the proton beam densities, are parametrized by the two weights w_i and the four correlation parameters $\rho_{i,j}$.

For each element in this set, the one-dimensional x and y scan curves are fitted with a double-gaussian model and the beam overlap integral O_I is estimated based on the assumption on the factorizability in x - y of the bunch proton densities

$$O_I = \int_{-\infty}^{\infty} \rho_1(x)\rho_2(x) dx \times \int_{-\infty}^{\infty} \rho_1(y)\rho_2(y) dy. \quad (6)$$

To show the impact introduced by x - y dependencies in the beam-shapes on the VdM scan method, the relative difference of the true O_I and reconstructed overlap region of three different examples of random beam-shape samples is shown in Figure 1. For each beam-shape type the widths are varied within $\sigma_{N,x,y} \in [1.6, 1.8]$ and $\sigma_{W,x,y} \in [2.4, 2.6]$. The red histogram shows the case for which $w_i = 0$, $\rho_{1,j} = 0.2$ and $\rho_{2,j} = -0.2$, the case for which $w_i = 0.5$ and $\rho_{1,j} = 0$ is shown in the black histogram and the blue histogram shows the impact of putting $w_i = 0.5$ and $\rho_{i,j} = 0.2$.

Amongst these examples, the impact is largest for correlation parameters having the same-sign and $w_i = 0.5$, and reaches an up to 4% difference between the true and reconstructed beam overlap integral. This overestimation leads effectively to an underestimation of the luminometer cross section and biases luminosity measurements at collider experiments.

The four correlation parameters $\rho_{i,j}$ are experimentally constrained by horizontal and vertical beam emittance adjustments in particle accelerators. Large values can nevertheless not be fully excluded and can lead in extreme cases to biases as large as 10%.

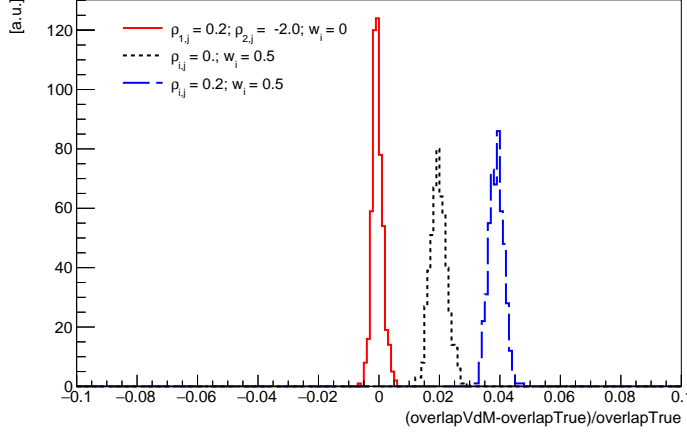


Figure 1: An estimate of the impact of x - y dependencies described in Equation 4 and 5 on the VdM scan method is shown. The blue histogram shows the relative difference between the reconstructed and true beam overlap integral for beam-shape parameters $w_i = 0.5$ and $\rho_{i,j} = 0.2$. The red histogram for beam-shape parameters $w_i = 0$, $\rho_{1,j} = 0.2$ and $\rho_{2,j} = -0.2$, and the black histogram shows the difference for $w_i = 0.5$ and $\rho_{i,j} = 0$.

3 Two-dimensional Beam Imaging

As was shown in the last section, the VdM Scan method results in significantly different estimates for the beam-beam overlap integral compared to the true one, if the bunch proton densities exhibit x - y dependencies. Therefore, sizeable systematic uncertainties were assigned by the CMS and ALICE Collaborations [4, 7] and a bias of up to 3% was found by the LHCb Collaboration [6].

A higher precision may be achieved by fully reconstructing both two-dimensional proton density distributions of the colliding bunches. A natural choice is to measure the vertex distributions in the transverse plane, which is proportional to the proton densities of the two colliding bunches. The density of the number of vertices at a given point (x, y) accumulated during a time interval ΔT and convolved with the vertex reconstruction resolution V is given by

$$n^{vtx}(x, y) = \rho_1(x, y)\rho_2(x, y) (\nu_{rev}\Delta TN_1N_2\sigma_p\epsilon^{vtx}) \otimes V, \quad (7)$$

where N_i ($\approx 10^{11}$) is the number of protons in the corresponding bunch, ν_{rev} is the revolution frequency, typically 11245 Hz, for a bunch in the LHC ring and ϵ^{vtx} is the vertex reconstruction efficiency. For typical VdM scan LHC run conditions, an inelastic proton-proton collision rate of 50 kHz can be assumed. With a special (zero-bias) trigger set-up, detectors at colliders experiments are able to record data per bunch crossing. For each scan point, data is typically collected within a time window of 25s. For the study in this paper, we therefore assume about 10^6 reconstructed vertices per scan.

During the Run-1 VdM scan campaigns [6], beam optics were chosen such that the beam width corresponds to $\sigma_b \approx 60 \mu m$, i.e. normalized transverse transmittance $\epsilon_N \approx 3 \cdot 10^{-7} m$ and $\beta^* \approx 11 m$,

$$\sigma_b = \sqrt{\epsilon_N \beta^*} \approx 60 \mu m. \quad (8)$$

The vertex reconstruction resolution V is dependent on the number of associated tracks and is about $\mathcal{O}(10) \mu m$ [15], and we assume therefore $\sigma_V \approx \frac{1}{3}\sigma_b$.

As described in the introduction an asymmetric scan setup is used as proposed in [12] and [13]. To derive the fit-model for the vertex distributions and without loss of generality the constants in Equation 7 are set to 1

$$\nu_{rev}\Delta TN_1N_2\sigma_p\epsilon^{vtx} := 1.$$

Considering a scan in x of one beam through the second in scan-steps Δx , the following equation holds

$$\sum_n n^{vtx}(x, y; n\Delta x)\Delta x = \sum_n \rho_1(x, y)\rho_2(x + n\Delta x, y)\Delta x \otimes V \quad (9)$$

$$= \left[\sum_n \rho_1(x, y)\rho_2(x + n\Delta x, y)\Delta x \right] \otimes V \quad (10)$$

$$\approx \left[\int_{\Delta x} \rho_1(x, y)\rho_2(x + \Delta x, y) d(\Delta x) \right] \otimes V \quad (11)$$

$$= \rho_1(x, y)(\mathcal{M}_x \rho_2)(y) \otimes V. \quad (12)$$

In the first step the distributivity property of convolutions is used and the approximation in the second step is the replacement of the sum over discrete scan points with a continuous integral over the beam-beam separation. After the integration, the x coordinate is integrated out and the bunch proton density of the moving beam appears marginalized in x .

Considering four scans of this kind, first scanning Beam 1 over Beam 2 in x and y and then vice versa, four two-dimensional vertex distributions are accumulated:

$$n_{x,2}^{vtx}(x, y) = \rho_2(x, y)(\mathcal{M}\rho_1(y)) \otimes V \quad (13)$$

$$n_{y,2}^{vtx}(x, y) = \rho_2(x, y)(\mathcal{M}\rho_1(x)) \otimes V \quad (14)$$

$$n_{x,1}^{vtx}(x, y) = \rho_1(x, y)(\mathcal{M}\rho_2(y)) \otimes V \quad (15)$$

$$n_{y,1}^{vtx}(x, y) = \rho_1(x, y)(\mathcal{M}\rho_2(x)) \otimes V. \quad (16)$$

Each distribution constrains different parts of the underlying beam proton densities. For example $n_{x,2}^{vtx}(x, y)$ only depends on Beam 2 in x and therefore fully constrains the width of Beam 2. Furthermore, this distribution has x - y dependencies if and only if there are x - y dependencies in the proton density of Beam 2. Together with $n_{y,2}^{vtx}(x, y)$ the proton density of Beam 2 is therefore fully constrained.

Assuming analytic models for $\rho_1(x, y)$ and $\rho_2(x, y)$ as well as the spacial vertex reconstruction resolution V , the four distributions can be fitted and the full two-dimensional proton densities of the two colliding bunches of Beam 1 and Beam 2 estimated.

For arbitrary beam shape models the convolution with the vertex reconstruction resolution is difficult and only possible by utilizing numerical convolution methods which in turn result in high performance inefficiencies time-wise. In past VdM scan campaigns however the bunch proton densities have been found to be sufficiently described by sums of gaussians [9] and the vertex reconstruction can equally well be approximated by a sum of gaussian resolution models. The application of deconvolution and unfolding methods in combination with the beam imaging should be investigated further.

Ten thousand beam imaging scans with 19 steps within the range of $\pm 4.5\sigma_b$ are simulated with double-gaussian beam shapes described in Eq. 4.

The fit model from Equation 13 is then used and fitted simultaneously to the four two-dimensional vertex distributions. We use package ROOFIT [16] to perform the fits. The beam shape input parameters are varied within the following ranges

$$w_{1,2} \in [0, 1] \quad \rho_{N,W} \in [-0.4, 0.4], \quad (17)$$

$$\sigma_{N,x,y} \in [1.6, 2.0] \quad \sigma_{W,x,y} \in [2.0, 2.6]. \quad (18)$$

Figure 4 shows a comparison of the true beam shape parameters and the best-fit parameters extracted from the simultaneous fit of the 4 vertex distributions using the fit-model derived in Equation 13.

The beam overlap is then estimated from the fit and compared to the true overlap calculated from the beam shape input parameters, as shown in Figure 5 (blue dashed histogram). A relative shift of approximately 1% is observed. This difference can be viewed as a systematic bias of the method and is corrected for with the procedure developed in the next section.

An example for a fit result is shown in Table 1. For this particular example the true beam overlaps and

the ones estimated with the VdM scan method are

$$\begin{aligned} O_I^{\text{true}} &= 0.0202, \\ O_I^{\text{BI}} &= 0.0202 \pm 0.0001, \\ O_I^{\text{VdM}} &= 0.0206 \pm 0.0001. \end{aligned}$$

While the beam imaging method measures a beam overlap consistent with the true beam overlap, a relative difference of about 2% is observed when the VdM scan method is applied to measure the beam overlap.

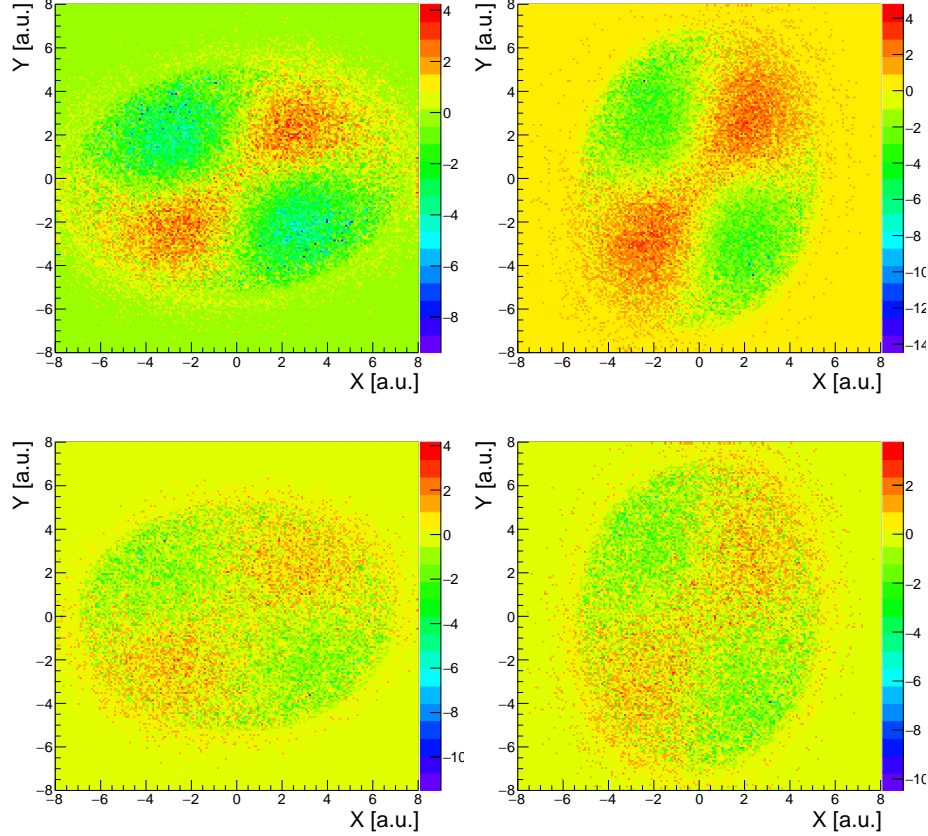


Figure 2: Pulls of the two fitted single gaussian beam-shapes to the four two-dimensional vertex distributions accumulated during simulated beam imaging scans. Beam 1 at rest and scanned with Beam 2 in x (top left), Beam 1 at rest and scanned with Beam 2 in y (top right), Beam 2 at rest and scanned with Beam 1 in x (bottom left), Beam 2 at rest and scanned with Beam 1 in y (bottom right).

Parameter	Input Beam 1	Fit Beam 1	Input Beam 2	Fit Beam 2
$\sigma_{W,x}$	2.358	2.319 ± 0.005	2.235	2.05 ± 0.01
$\sigma_{W,y}$	2.014	1.983 ± 0.006	2.377	2.14 ± 0.02
$\sigma_{N,x}$	1.874	1.881 ± 0.007	1.911	1.886 ± 0.007
$\sigma_{N,y}$	1.955	1.981 ± 0.006	1.93	1.89 ± 0.01
ρ_N	0.395	0.419 ± 0.003	0.063	0.011 ± 0.005
ρ_W	0.120	0.123 ± 0.005	0.30	0.21 ± 0.01
weight	0.521	0.482 ± 0.008	0.71	0.61 ± 0.04

Table 1: Example of fit results for one simulated beam imaging scan for Beam 1 and Beam 2. True double gaussian parameters and the parameters extracted from the beam imaging fit procedure with the statistical errors are shown.

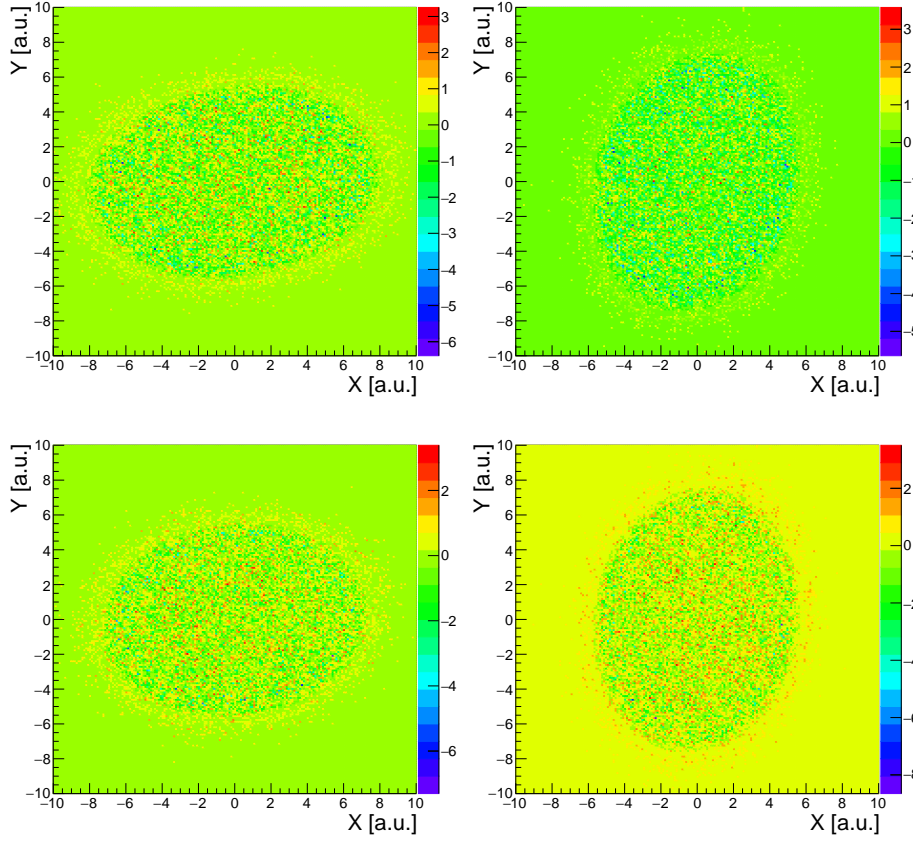


Figure 3: Pulls of the two fitted double gaussian beam-shapes to the four two-dimensional vertex distributions accumulated during simulated beam imaging scans. Beam 1 at rest and scanned with Beam 2 in x (top left), Beam 1 at rest and scanned with Beam 2 in y (top right), Beam 2 at rest and scanned with Beam 1 in x (bottom left), Beam 2 at rest and scanned with Beam 1 in y (bottom right). The best-fit parameters are shown in Table 1.

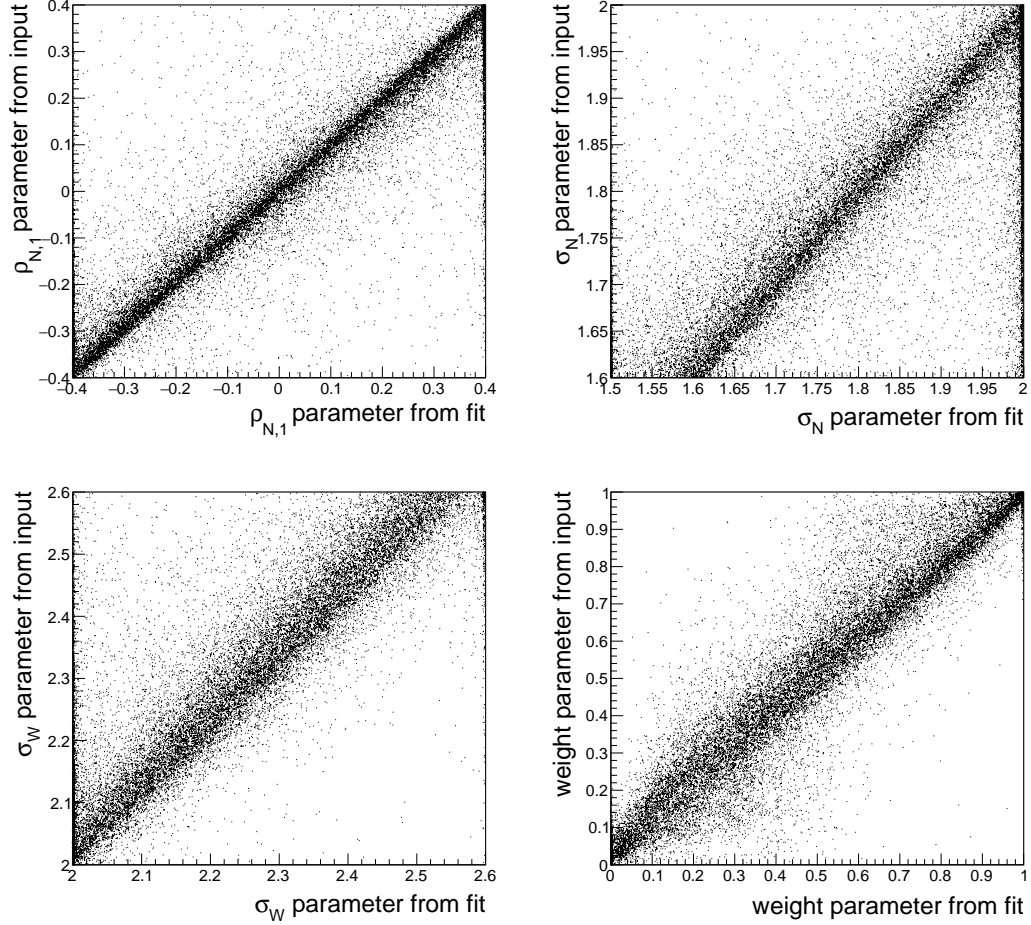


Figure 4: Examples of correlations between the fitted (x -axis) and true (y -axis) beam shape parameters are shown. Top left shows the correlation between the correlation parameters for the narrow double gaussian component of Beam1, top right shows the correlation between the width parameter for the narrow double gaussian component of Beam 1, bottom left shows the correlation between the width parameter for the wide double gaussian component of Beam 2 and the bottom right plot shows the correlation between the weight parameter for the double gaussian of fit model of Beam 1.

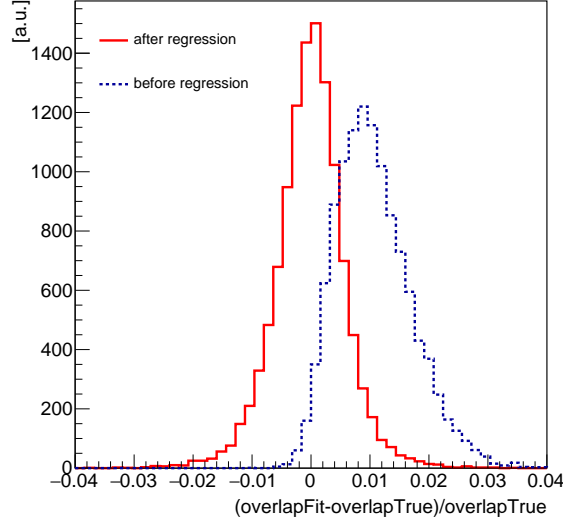


Figure 5: The relative difference of the true beam overlap and the reconstructed beam overlap using the beam imaging method before (blue dashed histogram) and after regression (red histogram) is shown.

4 Bias Study and Regression

A dedicated method to correct for the on average 1% shift in the reconstructed beam overlap is developed in this section. The method utilizes the regression functionalities based on neural networks of the TMVA package [17]. A regression for the beam overlap is trained using the fitted beam shape parameters as input variables targeting the true beam overlap integral computed from the input beam shape parameters

$$f^{\text{regression}} : S(P^{\text{fit}}) \longrightarrow S(O_I^{\text{true}}), \quad (19)$$

where $S(P^{\text{fit}})$ is the set of fitted parameters declared in Equation 17 and $S(O_I^{\text{true}})$ is the set of beam overlap integrals calculated from the input parameters of the bunch proton densities.

The sample of ten thousand simulated beam imaging scans is split into two random sub sets of samples with five thousand scans each. One sample is used to train the regression and the other one is used to evaluate the performance of the regression to prevent training bias.

The result is shown in Figure 5, red histogram. Compared to the uncorrected beam overlap, blue dashed histogram, the regression method improves the resolution to 0.6% and successfully removes the bias.

5 Conclusions

We discussed a method to reconstruct two-dimensional proton bunch densities using vertex distributions accumulated during LHC beam-beam scans. The x - y dependencies in the beam shapes are studied and an alternative luminosity calibration technique is introduced. Dependencies in x - y can lead to a significant overestimation of the instantaneous luminosity during the VdM scan and therefore bias the luminometer visible cross section estimate towards low values. With the beam imaging method introduced here, we measure x - y dependencies directly and hence the beam overlap integral for arbitrary beam shapes. In Section 3, we derive a fit model for two-dimensional vertex distributions in the transverse plane of a detector accumulated during beam imaging scans, where one beam is kept fixed and the other one is moved in x and y . We evaluate the method on a sample of simulated beam imaging scans with double gaussian beam shapes. After applying a dedicated correction based on a neural network regression technique the beam overlap integral is reconstructed with a precision of better than 1% assuming typical scan parameters.

6 Acknowledgments

We are grateful for the support of Catherine Medlock by the MIT-MISTI program and of Jakob Salfeld-Nebgen by the German Research Foundation. We would like to thank Colin Barschel and Marco Zanetti for fruitful discussions in the initial phase of this project.

References

- [1] S van der Meer. Calibration of the effective beam height in the ISR. Technical Report CERN-ISR-PO-68-31. ISR-PO-68-31, CERN, Geneva, 1968.
- [2] Carlo Rubbia. Measurement of the luminosity of $p\bar{p}$ collider with a (generalized) Van der Meer Method. Technical Report CERN-p \bar{p} -Note-38, CERN, Geneva, Nov 1977.
- [3] Simon White, Reyes Alemany-Fernandez, Helmut Burkhardt, and Mike Lamont. First Luminosity Scans in the LHC. *Conf. Proc.*, C100523:MOPEC014, 2010.
- [4] CMS Collaboration. CMS Luminosity Based on Pixel Cluster Counting - Summer 2013 Update. 2013.
- [5] Georges Aad et al. Improved luminosity determination in pp collisions at $\sqrt{s} = 7$ TeV using the ATLAS detector at the LHC. *Eur. Phys. J.*, C73(8):2518, 2013.
- [6] Roel Aaij et al. Precision luminosity measurements at LHCb. *JINST*, 9(12):P12005, 2014.
- [7] Betty Bezverkhny Abelev et al. Measurement of visible cross sections in proton-lead collisions at $\sqrt{s_{NN}} = 5.02$ TeV in van der Meer scans with the ALICE detector. *JINST*, 9(11):P11003, 2014.
- [8] M Ferro-Luzzi. Proposal for an absolute luminosity determination in colliding beam experiments using vertex detection of beam-gas interactions. *Nucl. Instrum. Methods Phys. Res., A*, 553(CERN-PH-EP-2005-023. 3):388–399. 17 p, May 2005.
- [9] Colin Barschel and Massimiliano Ferro-Luzzi. Precision luminosity measurement at LHCb with beam-gas imaging. 2014. Presented 05 Mar 2014.
- [10] Samuel Nathan Webb and Terry Wyatt. *Factorisation of beams in van der Meer scans and measurements of the ϕ_η^* distribution of $Z \rightarrow e^+e^-$ events in pp collisions at $\sqrt{s} = 8$ TeV with the ATLAS detector*. PhD thesis, Manchester U., Jun 2015. Presented 19 May 2015.
- [11] H Bartosik and G Rumolo. Production of single Gaussian bunches for Van der Meer scans in the LHC injector chain. Aug 2013.
- [12] Vladislav Balagura. Notes on van der Meer Scan for Absolute Luminosity Measurement. *Nucl. Instrum. Meth.*, A654:634–638, 2011.
- [13] Marco Zanetti. Beams Scan based Absolute Normalization of the CMS Luminosity Measurement. CMS 2010 luminosity determination. 2011.
- [14] R. Aaij et al. Absolute luminosity measurements with the LHCb detector at the LHC. *JINST*, 7:P01010, 2012.
- [15] Chatrchyan et al. Description and performance of track and primary-vertex reconstruction with the CMS tracker. *J. Instrum.*, 9(arXiv:1405.6569. CERN-PH-EP-2014-070. CMS-TRK-11-001):P10009. 80 p, May 2014.
- [16] Wouter Verkerke and David P. Kirkby. The RooFit toolkit for data modeling. *eConf*, C0303241:MOLT007, 2003. [,186(2003)].
- [17] Andreas Hoecker, Peter Speckmayer, Joerg Stelzer, Jan Therhaag, Eckhard von Toerne, and Helge Voss. TMVA: Toolkit for Multivariate Data Analysis. *PoS*, ACAT:040, 2007.